Equilibria and Dynamics for Mixed Vapors of BTX in an Activated Carbon Bed

Jeong-Ho Yun and Dae-Ki Choi
Environment & Process Technology Div., Korea Institute of Science & Technology, Seoul 130-650, Korea

Sung-Hyun Kim
Dept. of Chemical Engineering, Korea University, Seoul 136-701, Korea

Experimental and theoretical studies were made on the adsorption of benzene, toluene, p-xylene, and their binary and ternary mixtures by activated carbon in an isothermal condition of 303 K. Experimental isotherms for pure components were measured by two kinds of experimental techniques: the static volumetric method and breakthrough data analysis. Breakthrough data analysis shows that both the extended Langmuir equation and the ideal adsorbed solution theory could explain mixture isotherm data with good accuracy. In addition, a mathematical model was developed to simulate the column dynamics of pure and mixed-vapor adsorption systems. To represent the mass-transfer rate inside the adsorbent particle, the linear driving-force approximation model was applied. By optimizing the pure- and the binary-component breakthrough curve data with a dynamic model, an empirical correlation was proposed to represent the overall mass-transfer rates for the BTX vapor-activated carbon system. Results with this correlation, which is a function of the partial pressures for each adsorbate and interstitial bulk fluid velocities, showed that the prediction agrees well with the experimental data of ternary breakthrough curves.

Introduction

Adsorption has been widely recognized as an effective means of controlling emissions to the atmosphere and, in some applications, of recovering recyclable materials from process exhaust streams. A particularly common application of adsorption is solvent recovery. The most generally used adsorbent for solvent recovery systems for gas streams is activated carbon. Activated carbon has been generally used as a promising adsorbent, because it possesses a high surface area, an intricate pore structure, and a hydrophobic nature.

To design the adsorptive separation processes, it is important to understand the thermodynamic equilibrium relations and kinetic characteristics between the adsorbent used and adsorbates. However, there appears to be relatively little information in the literature concerning multicomponent adsorption of aromatic hydrocarbons on activated carbon at room temperature. In general, thermodynamic information on adsorption equilibrium can be obtained by the conventional measurement techniques such as the static volumetric and the static gravimetric methods (Valenzuela and Myers, 1989). Besides, the kinetic information, such as transport properties in the apparatus and intraparticle diffusion mechanisms, can be extracted from the column experiments with the changeable operating variables (that is, fluid velocity, concentrations, temperatures). However, for some solvents, which are relatively high boiling hydrocarbons, experimental difficulties might be involved in the adsorption equilibrium measurements. For example, these measurements could be affected because such hydrocarbons can easily be condensed in the equilibrium apparatus even at low partial pressures. In addition, equilibrium measurements for compounds exhibiting very high affinity for the adsorbent are quite difficult to make in practice (Paludetto et al., 1987), as in the case of aromatic hydrocarbons on activated carbon. In this regard, several efforts have been made to measure adsorption equilibrium and kinetic information simultaneously by analyzing the breakthrough curve data (Busmundrud, 1993; Takeuchi and Shigeta, 1991; Takeuchi et al., 1995). Such a method has another advantage in that it can be used to obtain the informa-

Correspondence concerning this article should be addressed to J.-H. Yun.

tion on multicomponent adsorption systems without difficulty.

In the present study, we focused our attention on investigating the equilibrium relationships and the kinetic information on the mixed-vapor adsorption systems of benzene, toluene, and *p*-xylene with commercial activated carbon. Benzene, toluene, and *p*-xylene (BTX) are ubiquitous materials in many industrial fields. Furthermore, it has been reported that these aromatic hydrocarbons are neurotoxic, and consequently cause diseases of the nervous system and sterility (White and Proctor, 1997).

Pure-component isotherms were measured by two different experimental techniques: isothermal column experiment and the static volumetric method. Adsorption equilibrium isotherms of binary and ternary mixtures were obtained by breakthrough curve analysis. It was found that the multicomponent equilibrium results were predicted satisfactorily by both the extended Langmuir equation and the ideal adsorbed solution theory. In addition, a mathematical model was applied to predict the multicomponent dynamic behavior. The model is based on the extended Langmuir equation as a multicomponent isotherm and the linear driving force expression for the diffusion resistance to mass transfer. By optimizing the pure and binary component breakthrough curve data with a mathematical model, the effective overall mass-transfer coefficients with changeable operating variables were obtained and represented by an empirical correlation. This correlation, which is a function of the partial pressures of adsorbates and interstitial bulk fluid velocities, yielded reasonable predictions compared with the experimental data of ternary breakthrough curves.

Experimental Studies

Pure-species isotherms

As an adsorbent, Sorbonorit B activated carbon (Norit Co.) was chosen, and its 12- and 14-mesh ratio was used after crushing. Prior to equilibrium measurement, the sample was kept in a drying vacuum oven at 423 K for over 24 h to remove impurities. To determine the equilibrium isotherms for pure species at 303 K, two kinds of experimental techniques were employed. For benzene and toluene vapors, the equilibrium isotherms were measured by using a static volumetric apparatus. Details of a static volumetric apparatus and the operating procedures used appear in the previous publications of Yun et al. (1998a,b). For *p*-xylene vapor, however, it was practically impossible to measure an equilibrium isotherm by a static volumetric method because of the high affinity for activated carbon and low vapor pressure at room temperature. We therefore utilized the column experiment to obtain the equilibrium isotherm for *p*-xylene; a detailed description of this method is presented in the following subsection.

Fixed-bed experiments

Fixed-bed adsorption has been widely applied in many fields of separation and purification. When dealing with a multicomponent system, the performance of a fixed bed is evaluated by examining the concentration vs. time curves of the effluent. Even for the cases in which one needs to know the effluent histories for a certain species only, it is necessary to obtain them all because of the interactions between the adsorbable components. These breakthrough curves have been considered the most common basis for the assessment of the behavior of adsorbers (Park and Knaebel, 1992; Tien, 1994).

If the adsorbable species exist at the trace level and the flow rate and temperature are constant during the experiment, one can calculate the amount adsorbed at a specific equilibrium concentration (inlet concentration) as follows:

$$N_i = \frac{FC_{i0}}{w}\left[t_s - \int_0^{t_s} \frac{C_i}{C_{i0}}\,dt\right], \tag{1}$$

where N_i is moles adsorbed of species i; F is volume flow rate; C_i is exit concentration of species i; C_{i0} is the inlet concentration of species i; w is mass of adsorbent; and t_s is saturation time (that is, the elapsed time when all C_i reach C_{i0} at the exit of the column).

In this study, to obtain the information on adsorption equilibrium relationships, many sets of fixed-bed experiments were very carefully conducted. Figure 1 shows the apparatus used. The nitrogen gas line was divided into five branches. One is for pure nitrogen gas as a carrier, and the others are connected to four branched solvent saturators. In the method, a part of the nitrogen gas was fed to a saturator to load the objective solvent, and was mixed with the pure nitrogen gas stream. In order to ensure homogeneous mixing of the solvent vapors with a pure nitrogen gas stream, the static in-line mixer was installed at the inlet section of the adsorption column. With constant concentration, constant flow rate, and constant temperature, the solvents-laden gas stream was fed to a fixed-bed adsorption column. The system pressure was monitored by a pressure manometer, which was installed above the static mixer. All gas flow rates were metered and adjusted by five mass flow controllers. Experimental temperature was maintained by a circulating water bath, and its accuracy was ± 0.02°C at 303 K. About 10 g of dried activated carbon was packed in a stainless-steel column of 1.82 cm ID and a height of about 10 cm. During the adsorption, the concentration history at the exit of the adsorption bed was monitored by a gas chromatograph (Hewlett-Packard type 5890 series II) equipped with a flame-ionization detector. To analyze the concentration of effluent gas streams with a constant time interval, the automatic 6-port injection valve (Valco Co.) with digital timer (Autonics Type FX4) was used. To make sure of the accuracy of the adsorption isotherm collected by the fixed-bed method, the analysis was carried out with an exact time interval of between 3 and 5 min. A constant analysis time interval enables us to use Eq. 1 to easily calculate the adsorbed moles from breakthrough curves. After each adsorption experiment, a saturated adsorption column was regenerated for the next experimental run by admitting the pure nitrogen flow at 573 K for 12 h.

The properties of adsorbent and the packing characteristics of adsorption column are given in Table 1. Inlet concentrations of solvent-laden gas were set, respectively, at from 100 ppm to 10,000 ppm for pure component, and from 100 ppm to 4,000 ppm for binary and ternary mixtures. The linear velocity of the gas stream varied between 0.3 and 0.5 m/s (that is, flow rate range is 6 to 12 L/min), which is the same condition as for a commercial solvent recovery system. All

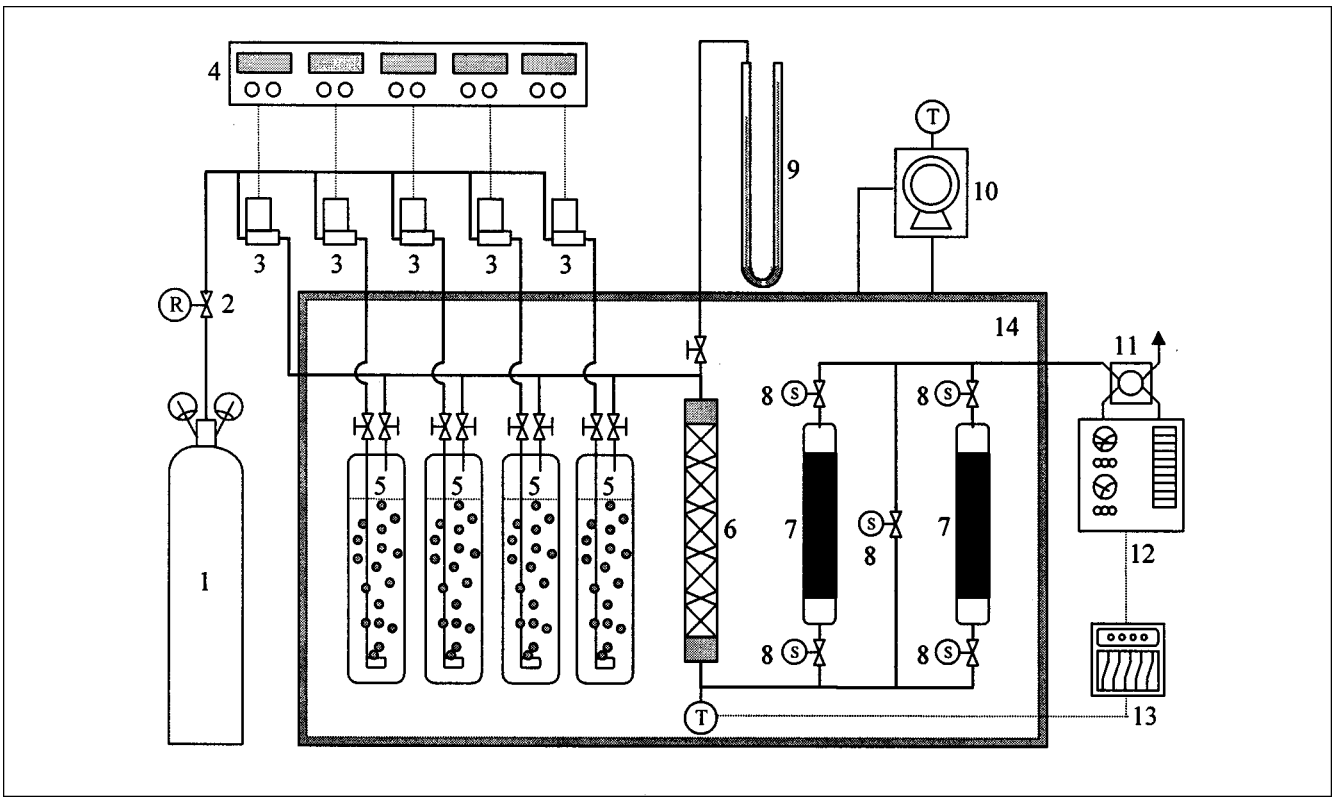

Figure 1. Experimental apparatus (ISOBED).

1. Nitrogen gas; 2. inlet pressure regulation valve; 3. mass flow meter; 4. control box; 5. solvent evaporator; 6. static mixer; 7. adsorption column; 8. solenoid ball valve; 9. manometer; 10. refrigerating/heating water circulator; 11. auto injection valve; 12. gas chromatography; 13. recorder; 14. constant temperature water bath.

experimental conditions for the binary and ternary adsorption systems are tabulated in Table 2.

Theoretical Considerations

Adsorption equilibrium

When dealing with a multicomponent adsorption system, reliable predictions of the adsorption equilibria are essential to properly analyze the dynamic behaviors of the adsorptive separation processes. For many decades, therefore, many efforts have been focused on developing the adsorption theories for predicting multicomponent adsorption equilibria using pure-component isotherm information. One of the simplest models for predicting multicomponent adsorption equilibria is the extended Langmuir equation (Ruthven, 1984; Yang, 1987). The advantage of this model is that the expression for equilibria is analytical and explicit, hence making the

Table 1. Properties of Adsorbent and Packing Characteristics

Adsorbent	Sorbonorit B (Norit Co.) 12–14 Mesh
BET surface area, $m^2 \cdot g^{-1}$	1,100–1,200
Particle density, $kg \cdot m^{-3}$	720
Bulk density, $kg \cdot m^{-3}$	400
Particle porosity	0.67
Bed void fraction	0.44

Table 2. Fixed-Bed Adsorption Runs for Binary and Ternary System

Run No.	w/g	$u/m \cdot s^{-1}$	Feed C_i/ppm		
			Benzene	Toluene	*p*-Xylene
2bt1	10.06	0.795	217.7	3,015.0	
2bt2	10.04	0.790	660.6	2,558.0	
2bt3	7.834	0.783	1,278.0	1,959.0	
2bt4	10.02	0.775	1,938.0	1,299.0	
2bt5	10.04	0.879	2,617.0	615.7	
2bt6	10.06	0.890	3,040.0	195.1	
2bx1	10.42	0.661	328.0		3,069.0
2bx2	10.41	0.679	735.4		2,664.0
2bx3	10.42	0.683	1,400.0		1,978.0
2bx4	10.41	0.692	2,012.0		1,394.0
2bx5	10.42	0.693	2,731.0		660.0
2bx6	10.41	0.851	3,175.0		220.0
2tx1	10.02	0.719		148.0	3,055.0
2tx2	10.05	0.758		617.0	2,581.0
2tx3	10.02	0.748		1,346.0	1,871.0
2tx4	10.02	0.741		1,966.0	1,237.0
2tx5	10.02	0.736		2,592.0	622.1
2tx6	9.002	0.722		2,953.0	239.0
3btx11	10.02	0.643	640.1	1,561.0	1,084.0
3btx12	10.02	0.891	1,636.0	967.0	683.3
3btx13	10.05	0.859	2,677.0	397.1	280.3
3btx21	10.02	0.891	2,319.0	793.0	702.9
3btx22	10.02	0.892	1,366.0	2,054.0	404.0
3btx23	10.05	0.892	657.0	2,970.0	197.8
3btx31	10.01	0.880	2,786.0	1,692.0	200.2
3btx32	10.05	0.907	2,395.0	1,439.0	743.3
3btx33	10.01	1.007	1,402.0	849.2	2,399.0

dynamic calculation much faster. Therefore, the extended Langmuir equation has been the major model used in calculations of adsorber dynamics for multicomponent adsorption (Ruthven, 1984; Yang, 1987).

On the other hand, the ideal adsorbed solution theory (IAST), which is based on solution thermodynamics, also has been widely applied to predict the multicomponent adsorption equilibria. The basic equation for IAST can be written as (Myers and Prausnitz, 1965):

$$Py_i = x_i P_i^0(\pi), \tag{2}$$

where P is total pressure; y_i and x_i are the gas phase and the adsorbed phase mole fractions for component i, respectively; and π is the spreading pressure of the mixture. The standard state pressure, $P_i^0(\pi)$, is defined as the gas pressure when only component i is present, which corresponds to the spreading pressure of the mixture. From the Gibbs isotherm, the spreading pressure is given as

$$\frac{\pi A}{RT} = \Pi_i\left(P_i^0\right) = \int_0^{P_i^0} \frac{n_i^0\left(P_i^0\right)}{P_i^0}\, dP_i^0, \tag{3}$$

where, $n_i^0(P_i^0)$ is the pure-component isotherm. Since there is no area change on mixing for an ideal adsorbed mixture, it follows that

$$\frac{1}{n_T} = \sum_i \frac{x_i}{n_i^0\left(P_i^0\right)}. \tag{4}$$

For the Langmuir equation as a pure-component isotherm, together with the stoichiometric constraint (the sum of adsorbed phase mole fraction is unity), the following relations are obtained:

$$n_i^0 = \frac{m_i b_i P_i^0}{1 + b_i P_i^0} \qquad \text{(Langmuir equation)} \tag{5}$$

$$\sum_i x_i = \sum_i \frac{b_i P y_i}{\exp\left(\Pi_i / m_i\right) - 1} = 1. \tag{6}$$

In general, the preceding set of equations can be solved numerically using Newton's method. For faster calculation, alternative techniques, such as the FastIAS algorithm (OBrien and Myers, 1988; Valenzuela and Myers, 1989) and Padé approximation (Frey and Rodriques, 1994), can be applied.

Dynamic modeling

Analysis of the present experiments requires a model for a four-component system, in which three components (benzene, toluene, and *p*-xylene) are adsorbable and the fourth component (N_2) is inert. The adsorbable species existed at trace levels and adsorbed in an isothermal condition. We consider an isothermal and plug-flow system, in which pressure drop in the bed is negligible and there is no variation in the fluid velocity along the bed length. The adsorption equilibrium relationship is represented by the extended Langmuir equation because of its simplicity, and the mass-transfer rate inside adsorbent particle is given by linear driving force (LDF) rate expression. With the ideal-gas law assumption, the set of equations for describing the present system is as follows:

Mass Balance for Component i:

$$-D_L \frac{\partial^2 y_i}{\partial z^2} + u\frac{\partial y_i}{\partial z} + \frac{\partial y_i}{\partial t} + \frac{RT}{P}\frac{1-\epsilon}{\epsilon}\rho_p \frac{\partial n_i}{\partial t} = 0. \tag{7}$$

Mass-Transfer Rates:

$$\frac{\partial n_i}{\partial t} = k_i\left(n_i^0 - n_i\right) \tag{8}$$

Adsorption Equilibrium:

$$n_i^0 = \frac{m_i b_i P y_i}{1 + \sum_i b_i P y_i}. \tag{9}$$

Boundary Conditions at $z = 0$ and $z = L$ and for $t > 0$:

$$D_L \left.\frac{\partial y_i}{\partial z}\right|_{z=0} = -u\left(y_i|_{z=0^-} - y_i|_{z=0^+}\right) \tag{10}$$

$$\left.\frac{\partial y_i}{\partial z}\right|_{z=L} = 0. \tag{11}$$

Although the model equation included the axial dispersion coefficient, plug flow was approximated by assigning a very large value to the Peclet number (uL/D_L). This is because the effect of axial dispersion is quite negligible in a small column and the model with the second derivatives can give more stable numerical results. The preceding set of partial differential equations (PDEs) was written in dimensionless form and the solution was numerically obtained. The PDEs were first reduced to a set of ordinary differential equations (ODEs) by the method of lines (MOL) technique, and the resultant ODEs were integrated with respect to time by using the subroutine DIVPAG in IMSL.

Results and Discussion

Equilibrium isotherms

Figure 2 shows pure adsorption equilibrium isotherms for benzene, toluene, and *p*-xylene vapors on activated carbon at 303 K. In this figure, the open symbols indicate the data obtained by the static volumetric method, and the closed symbols indicate the data obtained from the breakthrough data analysis, respectively. As can be seen, the qualitative agreements of two different experimental techniques are found in the benzene and toluene data. In the case of *p*-xylene, the experimental isotherm was only available by the column experiments because of its experimental difficulties, which are described in the experimental section. The experimental isotherms for each species were fitted with the Langmuir equation, and the isotherm parameters used are given in Table 3. As shown in Figure 2, the Langmuir equation is in good agreement with the experimental data for all three species. From the pure-component isotherms, it can be clearly stated that the order of adsorption affinities for BTX on activated carbon is *p*-xylene, toluene, and benzene. For maximum adsorption capacities, however, the order is toluene, benzene, and *p*-xylene in the experimental pressure range.

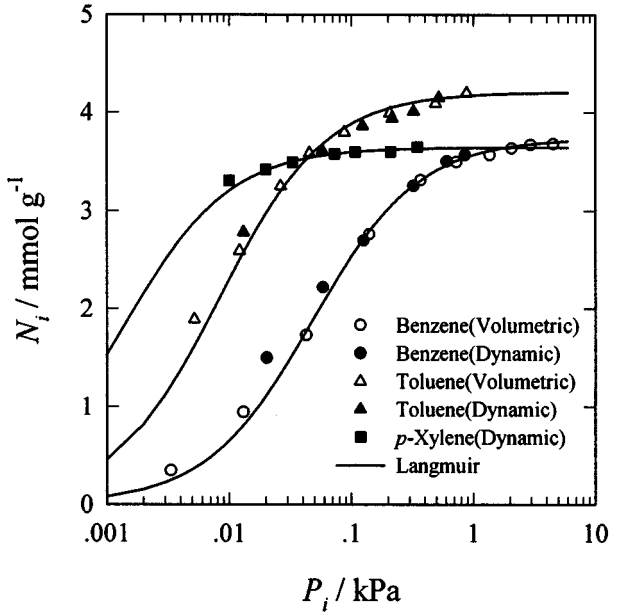

Figure 2. Equilibrium isotherms of benzene, toluene, and *p*-xylene on activated carbon at 303 K.

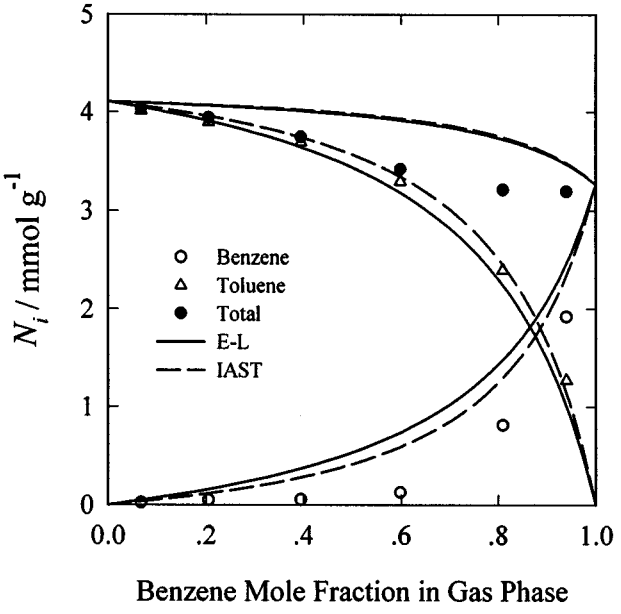

Figure 3. Equilibrium diagram for binary mixture of benzene and toluene on activated carbon at 303 K with constant total pressure of 0.327 kPa.

As discussed in the previous sections, all equilibrium data for binary and ternary mixtures were collected by performing several sets of column experiments. In addition, because of the convenience of their theoretical analysis, all experiments for mixtures were carried out with constant total concentration. It was done by adjusting the feed rates of nitrogen gas, which are connected to each saturator. During the experimental run, the system pressure was maintained at atmospheric condition. Since the adsorption of nitrogen on activated carbon is quite negligible, the actual concentrations of adsorbable species (solvent vapors) always existed at trace levels.

In this study, three pairs of binary mixtures were considered: benzene/toluene, benzene/*p*-xylene, and toluene/*p*-xylene. First, at a total concentration of about 3,230 ppm (same as 0.327 kPa in pressure), the adsorption equilibrium relationships for the benzene/toluene binary mixture on activated carbon were obtained as shown in Figure 3. These results were extracted by analyzing the breakthrough data of Runs 2bt1 to 2bt6, which are tabulated in Table 2. As mentioned in the experimental section, Eq. 1 was used to calculate the equilibrium amount adsorbed. In this figure, the open symbols indicate the amounts adsorbed for each species and the closed symbol indicates the total amount adsorbed. In addition, the prediction results using the extended Langmuir (E-L) equation are represented by the solid line, and those using the IAST are represented by the dashed line. As can be seen, the IAST gives slightly more accurate results than does the E-L equation, for the amount of toluene adsorbed. However, both equilibrium models fail to predict benzene and the total amount adsorbed. For the benzene/*p*-xylene binary mixture, the equilibrium data were obtained in a similar manner from the breakthrough data of Runs 2bx1 to 2bx6. The experimental results are shown in Figure 4 at a total concentration of 3,400 ppm (0.344 kPa). As shown in this figure, the adsorption affinity of *p*-xylene is much higher than that of benzene. In addition, the predictions using both the E-L equation and the IAST show nearly the same results. Furthermore, the accuracy of the E-L equation was excellent. The adsorption equilibrium relationships for the toluene/*p*-xylene binary mixture at a total concentration of 3,200 ppm (0.325 kPa) are shown in Figure 5. These results were obtained from the breakthrough data of Runs 2tx1 to 2tx6. As shown in this figure, the total amount of this binary mixture adsorbed increases slightly as the vapor mole fraction of toluene is increased. This is because the equilibrium amount of toluene adsorbed is greater than that of *p*-xylene at this equilibrium concentration. As can be seen, the E-L equation gives better prediction results than the IAST, except for the total amount adsorbed.

Table 3. Langmuir Equation Parameters for Benzene, Toluene, and *p*-Xylene on Activated Carbon at 303 K

Parameters	Benzene	Toluene	*p*-Xylene
m_i mmol/g	3.7367	4.2082	3.6447
b_i 1/kPa	20.992	120.14	723.84

The adsorption equilibria for the ternary mixture cannot be easily displayed as two- or three-dimensional plots. Therefore, previous works on ternary mixtures have usually performed along with constant pressure and composition paths because of their convenience (Costa et al., 1981; Gamba et al., 1990; Reich et al., 1980; Talu and Myers, 1988; Talu and Zwiebel, 1986; Yun et al., 1996). In this study, three sets of ternary adsorption systems were considered at different total constant concentrations (pressures), and each set was extracted from three sets of breakthrough data. Figure 6 shows the first set of equilibrium isotherms for the ternary mixture,

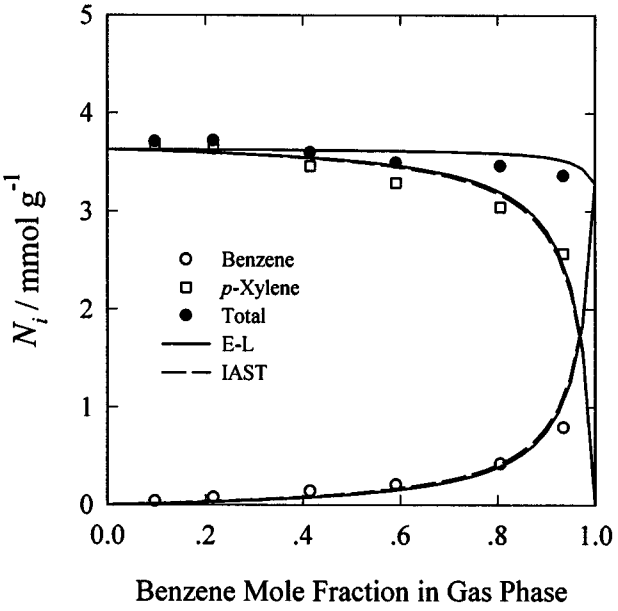

Figure 4. Equilibrium diagram for binary mixture of benzene and *p*-xylene on activated carbon at 303 K with constant total pressure of 0.344 kPa.

which was collected from breakthrough data of Runs 3btx11 to 3btx13. These results were obtained along the benzene mole fraction in the gas phase at a total constant concentration of 3,300 ppm (0.335 kPa). For each species, the E-L equation predicts the experimental results more accurately than does the IAST. However, both the E-L equation and the IAST give nearly the same results for benzene and the total amount adsorbed. In Figure 7, the second set of equilibrium isotherms is presented along with the toluene mole fraction in the gas phase at a total concentration of 3,820 ppm (0.387 kPa), as are the results collected from the breakthrough data of Runs 3btx21 to 3btx23. As shown in this figure, the E-L equation predicts the experimental data for toluene and *p*-xylene with better accuracy than does the IAST. It should be noted, however, that the IAST also gives good prediction results for both benzene and the total amount adsorbed. Finally, the last set of ternary isotherm data was obtained from the breakthrough data of Runs 3btx31 to 3btx33 at a total concentration of 4,630 ppm (0.470 kPa). Equilibrium isotherms are presented in Figure 8, along with the *p*-xylene mole fraction in the gas phase. In this case, because of experimental limitations, the experimental results were available only up to 0.5 of the gas-phase mole fraction of *p*-xylene. By employing the E-L equation, we still achieved better prediction results than the IAST. However, the IAST still gives good predictions for benzene and the total amount adsorbed.

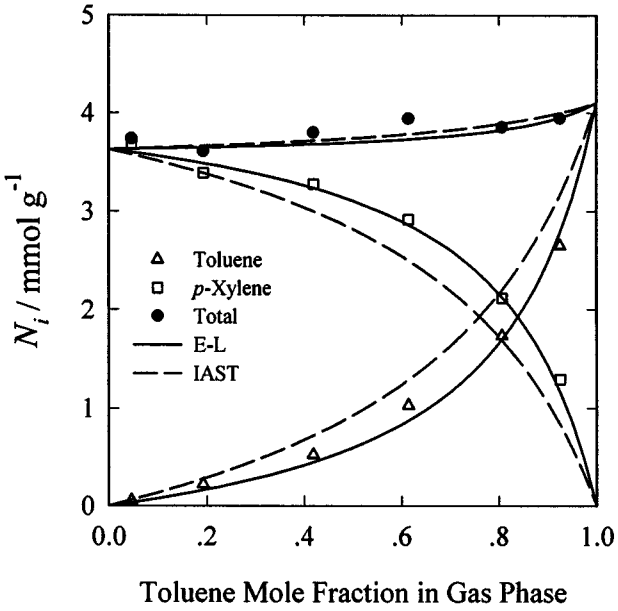

Figure 5. Equilibrium diagram for binary mixture of toluene and *p*-xylene on activated carbon at 303 K with constant total pressure of 0.325 kPa.

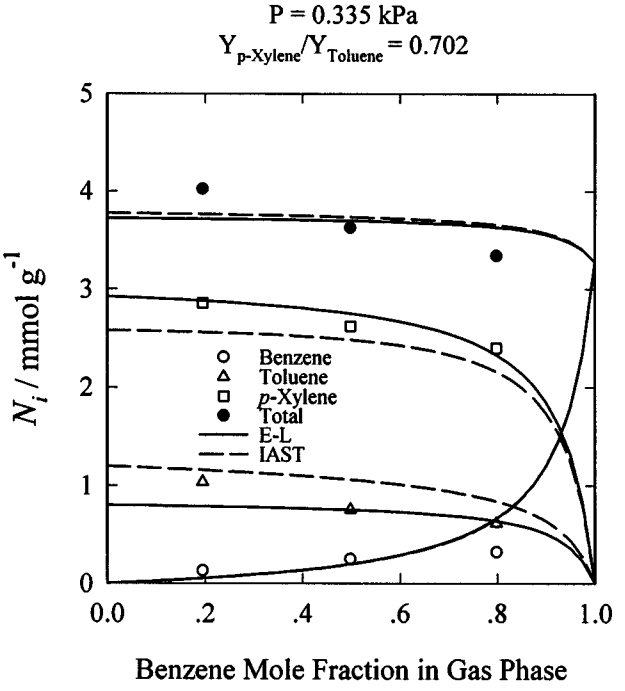

Figure 6. Equilibrium diagram for ternary mixture of benzene, toluene, and *p*-xylene on activated carbon at 303 K (data obtained from Runs 3btx11 to 3btx13).

From the results just shown, it can be concluded that the adsorption equilibria for binary and ternary mixtures of BTX could be satisfactorily predicted by pure-component equilibrium information. In other words, largely nonideal components, such as an azeotrope, were not found in the equilibrium diagram, and therefore its multicomponent adsorption behavior could be predicted with simple ideal models, such as the extended Langmuir equation and the ideal adsorbed solution theory. With respect to prediction accuracy, the E-L equation gives better results than the IAST for toluene and *p*-xylene. However, the IAST also gives good predictions for benzene and the total amount adsorbed. It was well known

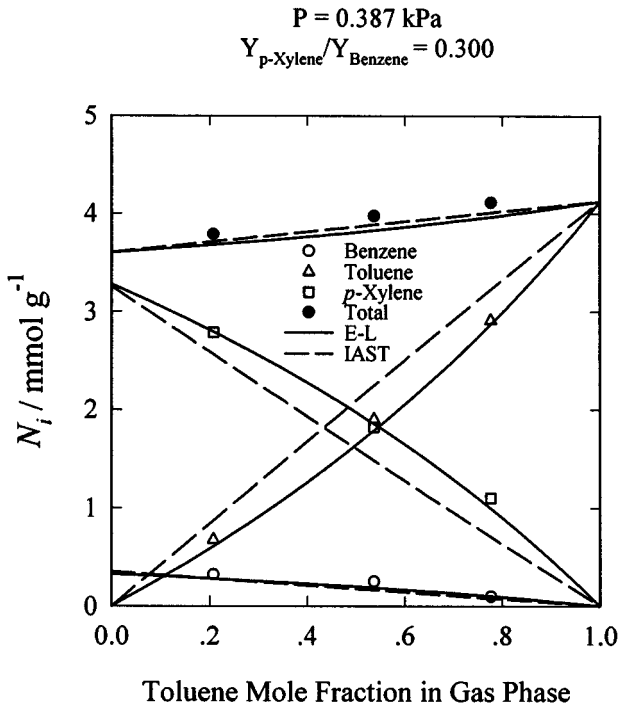

Figure 7. Equilibrium diagram for ternary mixture of benzene, toluene, and *p*-xylene on activated carbon at 303 K (data obtained from Runs 3btx21 to 3btx23).

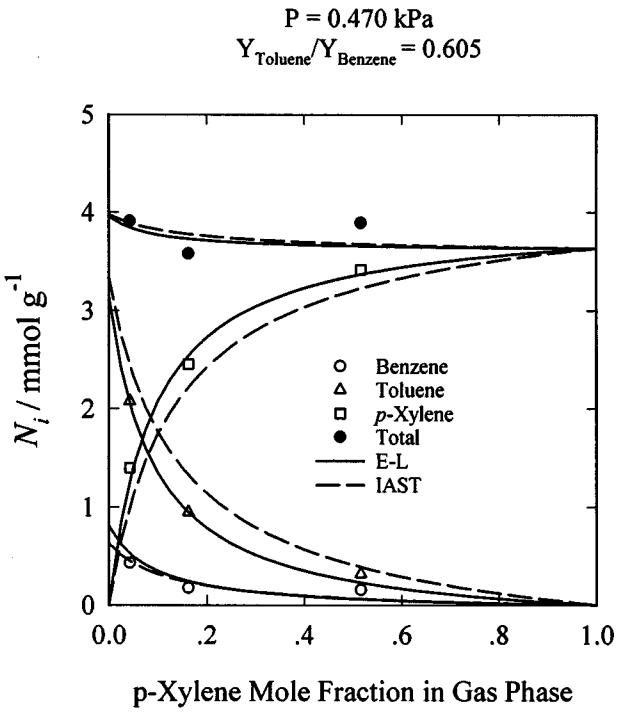

Figure 8. Equilibrium diagram for ternary mixture of benzene, toluene, and *p*-xylene on activated carbon at 303 K (data obtained from Runs 3btx31 to 3btx33).

that the success of the IAST relies on suitable pure-component equilibrium isotherms. Thus, it is believed that the failure of the IAST to predict toluene and *p*-xylene is due to the dearth of experimental isotherm data for pure components.

All experimental isotherm data for pure, binary, and ternary systems are given in the Appendix.

Column dynamics

When designing the adsorption facilities, one needs a reliable representation of the adsorption kinetics as well as the equilibrium isotherms for the adsorbent used. Information on the adsorption kinetics can be obtained by the mathematical modeling of an adsorption process. For isothermal adsorption, only the mass-transfer mechanism may be considerable. In general, the mass-transfer mechanism includes four steps: fluid film transfer, pore diffusion, adhesion on the surface, and surface diffusion. In order to quantitatively predict the dynamic behavior, complete solutions for each step are required. However, it is not easy to compute the multicomponent adsorption dynamics using a complete model, because of mathematical difficulties and the long computation time. For these reasons, the LDF approximation model for overall mass transfer has been widely applied to dynamic modeling. Many researchers have reported reasonable agreements between experimental data and models employing overall LDF mass-transfer coefficients (Basmadjian, 1980; Collins and Choa, 1973; Filippov, 1996; Huang and Fair, 1988; Mobidelli et al., 1982; Ruthven, 1984; Schork and Fair, 1988; Yang, 1987). Strictly speaking, the overall LDF mass-transfer coefficient is an effective lumped-resistance coefficient, and therefore it is important to investigate the effects of control variables on adsorption behaviors. In this study, the effects of two control variables, such as both the bulk fluid velocity and the concentrations (or partial pressures) for each solvent, were investigated.

As mentioned earlier, several sets of column experiments for pure and binary components were made. By using a mathematical model to optimize the breakthrough data of the pure and binary mixtures with the prediction results, the values of the overall LDF mass-transfer coefficients were obtained for various experimental conditions. By adapting a nonlinear regression technique, the results were correlated with the following relationship:

$$k_i = A_i P_i + B_i. \tag{12}$$

In Eq. 12, k_i are overall mass-transfer rate coefficients, and P_i are partial pressures for component *i*. In addition, A_i and B_i are specific parameters that are related to interstitial bulk fluid velocity in a packed column. All the parameters of A_i and B_i are listed in Table 4. Because of the lack of experimental data, the correlation cannot give a sufficiently usable range (that is, can only be available in the experimental

Table 4. Specific Parameters for Using the Eq. 12

Materials	A_i	B_i
Benzene	$0.609\times10^{-3}u+0.547\times10^{-2}$	$0.977\times10^{-3}u+0.104\times10^{-2}$
Toluene	$0.220\times10^{-1}u-0.890\times10^{-2}$	$0.271\times10^{-2}u-0.181\times10^{-2}$
p-Xylene	$-0.444\times10^{-2}u+0.811\times10^{-2}$	$0.135\times10^{-2}u-0.762\times10^{-3}$

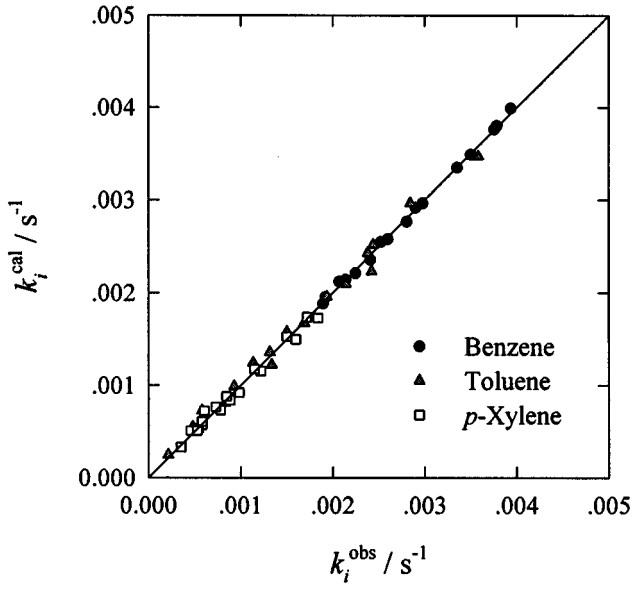

Figure 9. Comparison between measured overall mass-transfer coefficients and values calculated from Eq. 12.

range). The possible range is the partial pressure of 0.01 to 1.1 kPa for each species and the interstitial bulk fluid velocity of 0.66 to 1.0 m/s. A comparison between the observed values for k_i and the values calculated from Eq. 12 is shown in Figure 9.

Using this correlation, the experimental breakthrough curves for three pairs of binary mixtures were repredicted. The results are presented in Figure 10, and the experimental conditions for each run are presented in Table 2. In an equilibrium-controlled system, the phenomenon of "roll-up" is commonly observed in the breakthrough curves whenever the equilibrium relationship is favorable. Under these conditions, the more strongly adsorbed (and therefore slower traveling) species displaces the weaker (and faster traveling) species, leading, above the inlet value, to a rise in the effluent concentration of the less strongly adsorbed species. Such behavior is well understood (Farooq and Ruthven, 1991; Ruthven, 1984; Yang, 1987). For a binary mixture of benzene and toluene, toluene is better adsorbed than benzene, as shown in Figure 10A. Model predictions give qualitative agreements with experimental data; however, the model fails to predict the amount of roll-up for benzene. This is probably because the equilibrium model fails to predict the amount of benzene adsorbed in the benzene/toluene binary mixture. For both benzene/*p*-xylene and toluene/*p*-xylene binary mixtures, model predictions agree well with the experimental data, as shown in Figures 10B and 10C, respectively. In addition, it was found that if the concentration of strongly adsorbed species is lower, then saturation happens for a long time, as shown in the cases of Runs 2bt6, 2bx6, and 2tx6.

The experimental and predicted breakthrough curves for the ternary mixture are presented in Figure 11. Experimental conditions for each run are given in Table 2. As shown in this figure, model predictions agree well with the experimental ternary breakthrough curves. This implies that the suggested correlation for overall mass-transfer resistance is valid for the BTX adsorption system used for the activated carbon. Therefore, it can be expected that this correlation could be effectively used to design the adsorption facilities for using activated carbon in treating BTX vapors.

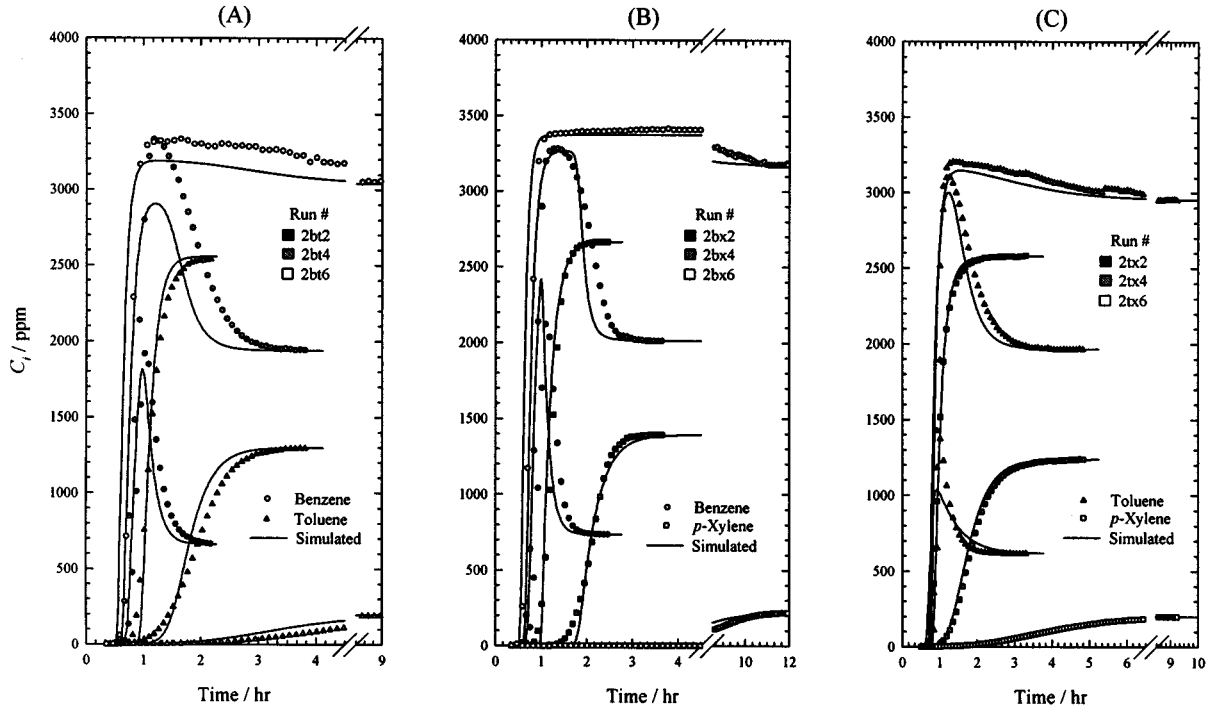

Figure 10. Experimental and predicted breakthrough curves for binary mixtures of BTX on activated carbon at 303 K.

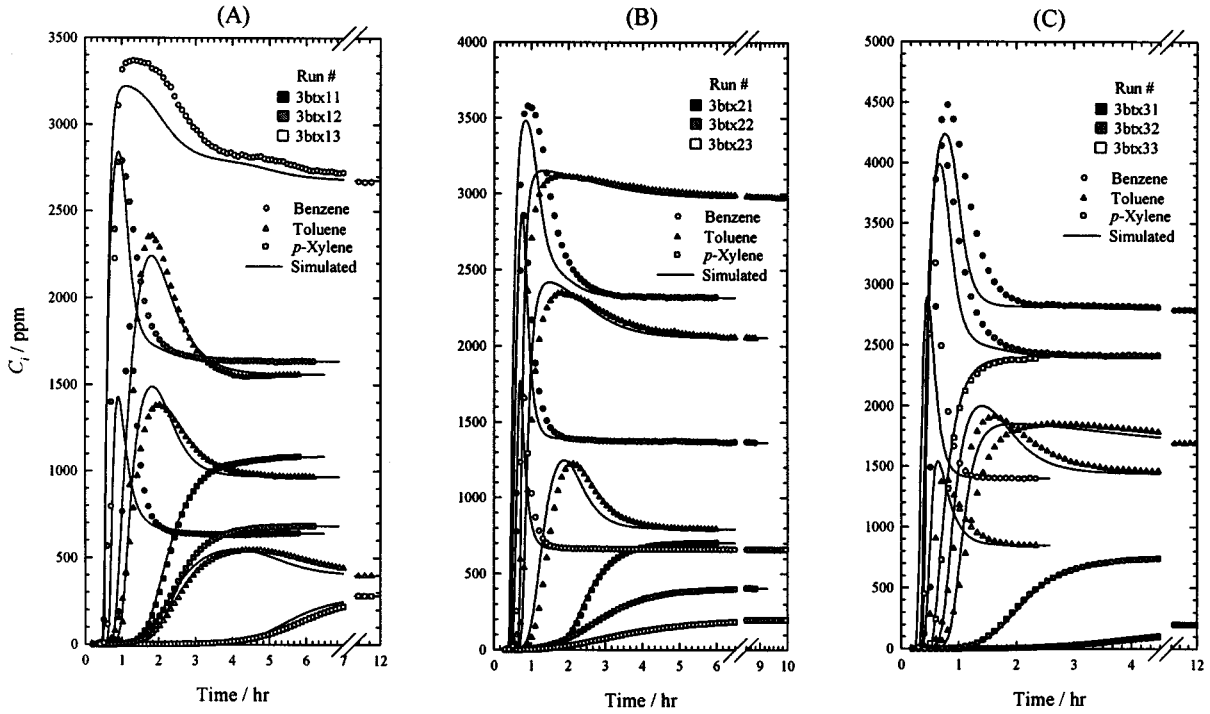

Figure 11. Experimental and predicted breakthrough curves for ternary mixture of BTX on activated carbon at 303 K.

Conclusions

In this study, many experiments were performed on the adsorption of mixed BTX vapors in activated carbon. For pure components, the adsorption equilibrium isotherms were measured by two experimental techniques: the static volumetric method, and breakthrough curve analysis. The results of the two different experimental techniques agreed well with each other qualitatively. For binary and ternary mixtures, the equilibrium relationships were obtained by breakthrough data analysis. The extended Langmuir (E-L) equation and the ideal adsorbed solution theory (IAST) agree well with the experimental isotherm data for binary and ternary mixtures. In addition, by using our dynamic model to analyze the pure and binary breakthrough data, an empirical correlation was suggested to the overall mass-transfer rates of BTX in a fixed bed that is charged with activated carbon. The validity of this correlation was proved by using the ternary breakthrough curve predictions. The experimental and theoretical results presented in this article will contribute to our future work on the removal of BTX from air by the cyclic operation of thermal swing adsorption (TSA). Furthermore, the adsorption equilibrium data in this study could be used to improve the theoretical models of the multicomponent adsorption equilibria of aromatic hydrocarbons in microporous solids.

Notation

b = Langmuir equation parameter, 1/kPa
D_L = axial dispersion coefficient
L = length of adsorbent bed, cm
m = Langmuir equation parameter, mmol/g
n = moles adsorbed, mmol/g
N_T = total moles adsorbed, mmol/g
n^0 = moles adsorbed at standard state, mmol/g
P_T = total pressure, kPa
P^0 = standard state pressure, kPa
R = gas constant
t = time, min
T = temperature, K
u = interstitial fluid velocity, m/s
Y = gas-phase mole fraction
z = axial distance
ϵ = bed void fraction
Π = modified spreading pressure
ρ_p = particle density, kg/m^3

Superscripts

cal = calculated value
obs = observed value

Literature Cited

Basmadjian, D., "Rapid Procedures for the Prediction of Fixed-Bed Adsorber Behavior. 2. Adiabatic Sorption of Single Gases with Arbitrary Isotherms and Transport Modes," *Ind. Eng. Chem. Proc. Des. Dev.*, **19**, 137 (1980).

Busmundrud, O., "Vapour Breakthrough in Activated Carbon Beds," *Carbon*, **31**, 279 (1993).

Collins, H. W., and K. Choa, "A Dynamic Model for Multicomponent Fixed Bed Adsorption," *AIChE Symp. Ser.*, **69**, 9 (1973).

Costa, E., J. L. Sotelo, C. Calleja, and C. Marron, "Adsorption of Binary and Ternary Hydrocarbon Gas Mixtures on Activated Carbon: Experimental Determination and Theoretical Prediction of the Ternary Equilibrium Data," *AIChE J.*, **27**, 5 (1981).

Farooq, S., and D. M. Ruthven, "Dynamics of Kinetically Controlled Binary Adsorption in a Fixed Bed," *AIChE J.*, **37**, 299 (1991).

Filippov, L. K., "Multicomponent Adsorption Dynamics of Polymers in a Fixed Bed," *Chem. Eng. Sci.*, **51**, 4013 (1996).

Frey, D. D., and A. E. Rodriques, "Explicit Calculation of Multicomponent Equilibria for Ideal Adsorbed Solutions," *AIChE J.*, **40**, 182 (1994).

Gamba, G., R. Rota, S. Carra, and M. Morbidelli, "Adsorption Equilibria of Nonideal Multicomponent Systems at Saturation," *AIChE J.*, **36**, 1736 (1990).

Huang, C.-C., and J. R. Fair, "Study of the Adsorption and Desorp-

tion of Multiple Adsorbates in a Fixed Bed,'' *AIChE J*., **34**, 1861 (1998).
Morbidelli, M., A. Servida, S. Glusepp, and S. Carra, ''Simulation of Multicomponent Adsorption Beds. Model Analysis and Numerical Solution,'' *Ind. Eng. Chem. Fundam*., **21**, 123 (1982).
Myers, A. L., and J. M. Prausnitz, ''Thermodynamics of Mixed Gas Adsorption,'' *AIChE J*., **11**, 121 (1965).
O'Brien, J. A., and A. L. Myers, ''A Comprehensive Technique for Equilibrium Calculations in Adsorbed Mixtures: The Generalized FastIAS Method,'' *Ind. Eng. Chem. Res*., **27**, 2085 (1988).
Paludetto, R., G. Storti, G. Gamba, S. Carra, and M. Morbidelli, ''On Multicomponent Adsorption Equilibria of Xylene Mixtures on Zeolites,'' *Ind. Eng. Chem. Res*., **26**, 2250 (1987).
Park, I., and K. S. Knaebel, ''Adsorption Breakthrough Behavior: Unusual Effects and Possible Causes,'' *AIChE J*., **38**, 660 (1992).
Reich, R., W. T. Ziegler, and K. A. Rogers, ''Adsorption of Methane, Ethane and Ethylene Gases and Their Binary and Ternary Mixtures and Carbon Dioxide on Activated Carbon at 212−301 K and Pressures to 35 Atmospheres,'' *Ind. Eng. Chem. Proc. Des. Dev*., **19**, 336 (1980).
Ruthven, D. M., *Principles of Adsorption and Adsorption Processes*, Wiley, New York (1984).
Schork, J. M., and J. R. Fair, ''Parametric Analysis of Thermal Regeneration of Adsorption Beds,'' *Ind. Eng. Chem. Res*., **27**, 457 (1988).
Takeuchi, Y., and A. Shigeta, ''Adsorption of Binary and Ternary Organic Solvent Vapor in Air by a Fixed Bed of Granular Activated Carbon,'' *J. Chem. Eng. Jpn*., **24**, 411 (1991).
Takeuchi, Y., H. Iwamoto, N. Miyata, S. Asano, and M. Harada, ''Adsorption of 1-butanol and *p*-Xylene and Their Mixtures with High Silica Zeolite,'' *Sep. Technol*., **5**, 23 (1995).
Talu, O., and I. Zwiebel, ''Multicomponent Adsorption Equilibria of Nonideal Mixtures,'' *AIChE J*., **32**, 1263 (1986).
Talu, O., and A. L. Myers, ''Rigorous Thermodynamic Treatment of Gas Adsorption,'' *AIChE J*., **34**, 1887 (1988).
Tien, C., *Adsorption Calculations and Modeling*, Butterworths, Boston (1994).
Valenzuela, D. P., and A. L. Myers, *Adsorption Equilibrium Data Handbook*, Prentice-Hall, Englewood Cliffs, NJ (1989).
White, R. F., and S. P. Proctor, ''Solvents and Neurotoxicity,'' *Lancet*, **349**, 1239 (1987).
Yang, R. T., *Gas Separation by Adsorption Processes*, Butterworths, Boston (1987).
Yun, J.-H., H.-C. Park, and H. Moon, ''Multicomponent Adsorption Calculations Based on Adsorbed Solution Theory,'' *Korean J. Chem. Eng*., **13**, 246 (1996).
Yun, J.-H., D.-K. Choi, and S.-H. Kim, ''Adsorption Equilibria of Chlorinated Organic Solvents onto Activated Carbon,'' *Ind. Eng. Chem. Res*., **37**, 1422 (1998a).
Yun, J.-H., D.-K. Choi, and S.-H. Kim, ''Adsorption of Organic Solvent Vapors on Hydrophobic Y-Type Zeolite,'' *AIChE J*., **44**, 1344 (1998b).

Appendix

The tables in this Appendix contain the adsorption equilibrium data for pure, binary, and ternary components of benzene, toluene, and *p*-xylene (BTX) vapors in activated carbon at 303 K.

Table A1. Pure-Component Equilibrium Data for Benzene, Toluene, and *p*-Xylene in Activated Carbon at 303 K

Volumetric Data*		Dynamic Data**	
P/kPa	N/mmol·g^{-1}	P/kPa	N/mmol·g^{-1}
Benzene		Benzene	
0.0033	0.3437	0.0202	1.4968
0.0131	0.9409	0.0585	2.2164
0.0428	1.7297	0.1258	2.6928
0.1403	2.7569	0.3237	3.2524
0.3709	3.3090	0.3248	3.2526
0.7259	3.4974	0.6082	3.5026
1.3680	3.5668	0.8575	3.5681
2.0653	3.6363		
2.9480	3.6730	Toluene	
4.5240	3.6800	0.0131	2.7790
Toluene		0.0580	3.6119
0.0052	1.8900	0.1235	3.8650
0.0121	2.5884	0.2154	3.9403
0.0264	3.2497	0.3243	4.0090
0.0456	3.5870	0.5226	4.1504
0.0880	3.7972	*p*-Xylene	
0.2071	3.9924	0.0100	3.3040
0.4911	4.0923	0.0199	3.4193
0.8837	4.1997	0.0330	3.4930
		0.0725	3.5792
		0.1076	3.5962
		0.2096	3.6019
		0.3461	3.6487

**Volumetric data* are the experimental equilibrium data obtained by the static volumetric method.
***Dynamic data* are the experimental equilibrium data obtained by breakthrough curve analysis.

Table A2. Experimental Equilibrium Data for Binary Mixtures on Activated Carbon at 303 K

Run No.	P_T/kPa	Y_1	X_1	N_T/mmol·g^{-1}
Benzene(1)−Toluene(2)				
2bt1	0.3276	0.0673	0.0051	4.0328
2bt2	0.3261	0.2052	0.0122	3.9404
2bt3	0.3280	0.3948	0.0137	3.7450
2bt4	0.3280	0.5987	0.0365	3.4194
2bt5	0.3276	0.8095	0.2527	3.2080
2bt6	0.3278	0.9397	0.6019	3.1902
Benzene(1)− *p*-Xylene(2)				
2bx1	0.3442	0.0966	0.0097	3.7087
2bx2	0.3444	0.2163	0.0210	3.7197
2bx3	0.3423	0.4144	0.0387	3.6002
2bx4	0.3451	0.5907	0.0591	3.4966
2bx5	0.3436	0.8054	0.1219	3.4638
2bx6	0.3440	0.9352	0.2367	3.3614
Toluene(1)− *p*-Xylene(2)				
2tx1	0.3245	0.0462	0.0137	3.7378
2tx2	0.3240	0.1929	0.0609	3.6095
2tx3	0.3260	0.4184	0.1373	3.7984
2tx4	0.3245	0.6138	0.2607	3.9407
2tx5	0.3257	0.8065	0.4500	3.8544
2tx6	0.3234	0.9251	0.6717	3.9441

Table A3. Experimental Equilibrium Data for the Ternary Mixture of Benzene(1), Toluene(2), and *p*-Xylene(3) on Activated Carbon at 303 K

Run No.	P_T kPa	Y_1	Y_2	X_1	X_2	N_T mmol·g^{-1}
3btx11	0.3329	0.1948	0.4752	0.0318	0.2579	4.0194
3btx12	0.3330	0.4979	0.2943	0.0689	0.2084	3.6266
3btx13	0.3398	0.7982	0.1184	0.0963	0.1841	3.3361
3btx21	0.3866	0.6079	0.2079	0.0846	0.1792	3.7863
3btx22	0.3875	0.3572	0.5371	0.0626	0.4790	3.9736
3btx23	0.3876	0.1718	0.7765	0.0232	0.7089	4.1084
3btx31	0.4740	0.5956	0.3617	0.1099	0.5317	3.9104
3btx32	0.4638	0.5233	0.3144	0.0488	0.2652	3.5802
3btx33	0.4712	0.3015	0.1826	0.0398	0.0817	3.8931

Manuscript received Sept. 22, 1998, and revision received Jan. 12, 1999.